# Imaging of the brachial and sacral plexus

Efrat Saraf-Lavi, MD

The brachial and sacral plexuses are networks of peripheral nerves responsible for innervation of the upper and lower limbs. Knowledge of the intrinsic anatomic structures and their relationship to adjacent muscles, vessels, and osseous landmarks is crucial for correct identification of normal plexus components and for the diagnosis of pathologic conditions.

Anatomy

The large peripheral nerves are composed of Schwann cell-axon complexes, supported and protected by 3 connective-tissue sheaths: endoneurium, perineurium, and epineurium. The innermost sheath, the endoneurium, surrounds each of the axon-Schwann cell complexes. The complexes are bundled into a fascicle, which is enclosed by the perineurium, a multilayered concentric connective tissue that acts as a protective barrier against disease along the fascicles. The epineurium, which is the outermost sheath, envelops the nerve and consists

Dr. Saraf-Lavi is an Associate Professor of Radiology at the University of Miami Miller School of Medicine, Miami, FL, and Medical Director of the Applebaum Diagnostic Imaging Center in Miami, FL.
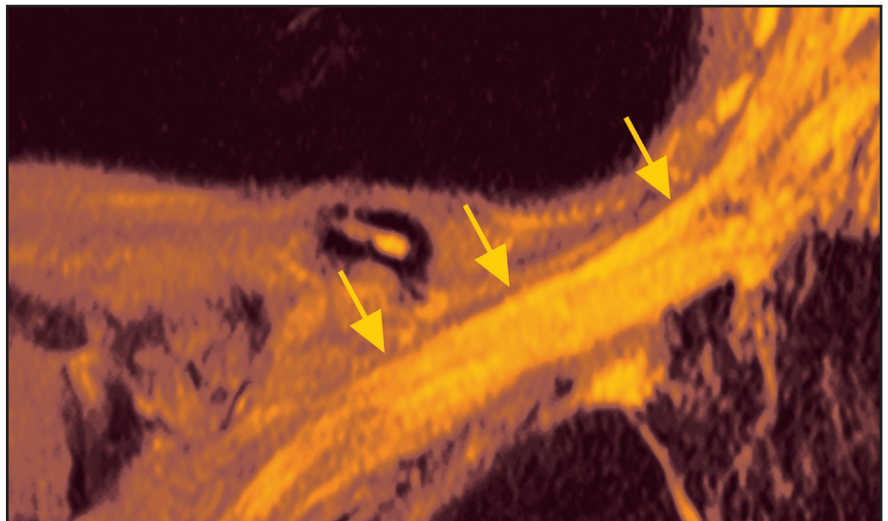
of dense connective tissue and thick collagen and elastin fibers.[1]

The brachial plexus is a network of peripheral nerves formed by the ventral rami (also referred to as "roots") of C5 through T1. The roots unite to form the upper (C5 and C6 roots), middle (C7 root), and lower (C8 and T1 roots) "trunks" in or near the cleft between the anterior and middle scalene muscles known as the interscalene triangle. The subclavian artery travels through the interscalene triangle with the plexus, while the subclavian vein courses anteriorly to the anterior scalene muscle. The trunks divide into anterior and posterior "divisions" just lateral to the interscalene tri-

angle. Subsequently, these divisions join to form three "cords" at or just lateral to the lateral margin of the first rib.[2,3] The anterior divisions of the upper and middle trunks form the lateral cord; the anterior division of the lower trunk forms the medial cord; and the posterior divisions form the posterior cord. The cords are named according to their position relative to the axillary artery. Near the lateral margins of the pectoralis minor muscle, each cord terminates in 2 major nerve branches (Figure 1).

The sacral plexus is formed from the ventral rami of L4/L5 (lumbosacral trunk) and S1 to S4. The roots divide into anterior and posterior divisions, which
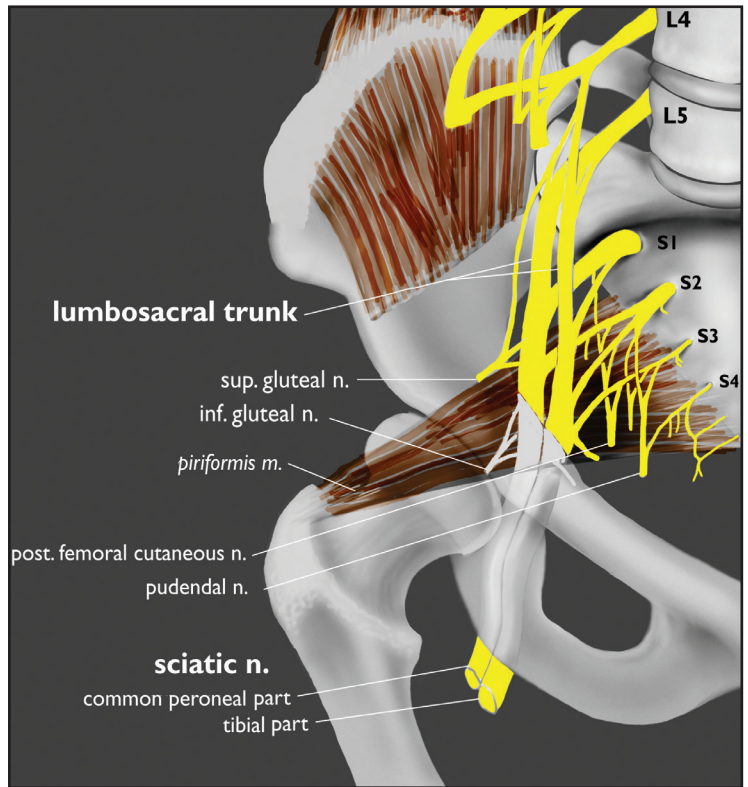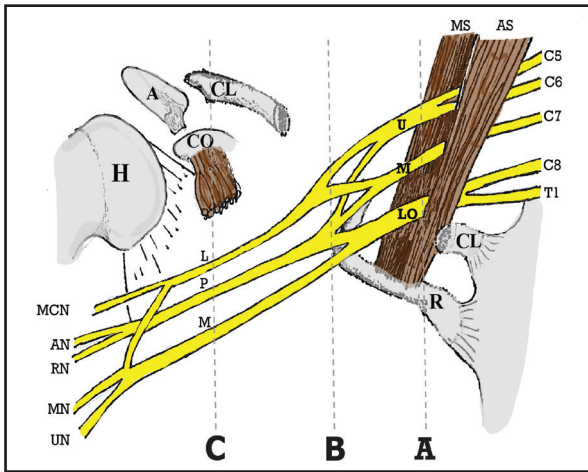
FIGURE 1. *Schematic drawing of the brachial plexus with selected musculoskeletal landmarks. The plexus is highlighted in yellow. The three dashed lines indicate sagittal planes that intersect the following landmarks: A- interscalene triangle, between the anterior scalene (AS) and middle scalene (MS) muscles; B- lateral margin of the first rib (R); and C- coracoid process (CO). Sagittal MR images corresponding approximately to planes A, B, and C are shown in Figure 4.The following plexus components are indicated: the roots forming the plexus (C5-T1), the three trunks (U- upper, M- middle and LO- lower) found on MRI at the level of the interscalene triangle, the anterior and posterior divisions found on MRI at the lateral margins of the first rib, the cords (L- lateral, P- posterior and M- medial) found on MRI at the level of the coracoid process and branches at the level of the axilla (MCN- musculocutaneous nerve, AN- axillary nerve, RN- radial nerve, MN median nerve, UN- ulnar nerve). A- acromion, CL- clavicle, and H-humerus.*

FIGURE 2. *Schematic drawing of the sacral plexus with selected musculoskeletal landmarks. The plexus is highlighted in yellow. The sacral plexus is formed from the ventral rami of l4, L5 (lumbosacral trunk) and S1-S4. The sciatic nerve (L4-S3) exits the pelvis through the greater sciatic foramen ventral to the piriformis muscle.*
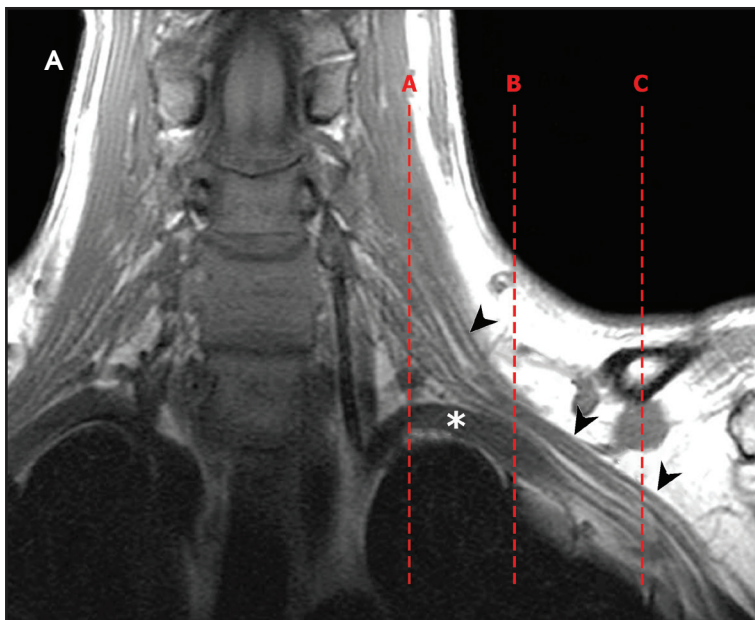

FIGURE 3. *Normal brachial plexus. (A) Coronal T1W image of a normal brachial plexus. The dashed lines indicate the approximate sagittal locations for the trunks (plane A), divisions (plane B) and cords (plane C) and correspond to the three sagittal planes in Figure 1. The brachial plexus (black arrowheads) is identified by its location superior to the "flow-void" of the subclavian artery (white asterisk) and appears as an elongated bundle of nerves, isointense to muscle interspersed with thin fat planes. (B) Sagittal T1W image at the level of the cords shows the rounded cords (black arrows) encompassing the axillary artery (A) from superior (lateral cord-L) to posterior (posterior cord-P) to inferior (medial cord - M) in clockwise order.*
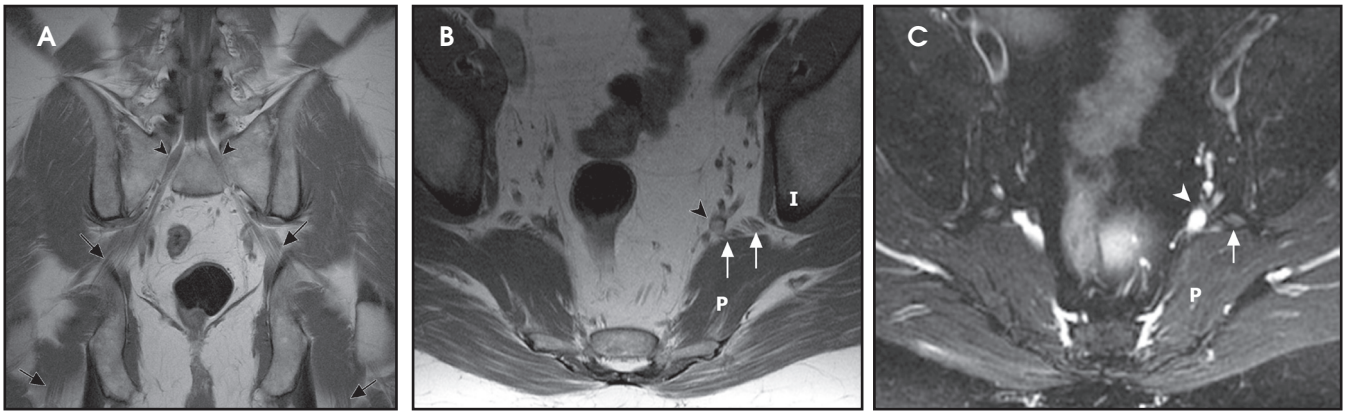
FIGURE 4. *Normal sacral plexus. (A) Coronal T1W image shows the bilateral S1 roots (arrowheads), sacral plexus and sciatic nerve (arrows). For each side, these components appear as continuous structures with a fine, striated appearance. (B) Axial T1W image at the level of the greater sciatic foramen shows the sacral plexus components (lumbosacral trunk and S1-S3) as clustered linear segments (arrows) anterior to the piriformis muscles (P), posterior to the ischium (I), and lateral to the inferior gluteal vessels (arrowhead). Slightly inferior to this section, the plexus components form the sciatic nerve, which exits the pelvis through the greater sciatic foramen. (C) Corresponding T2W image with fat suppression shows the normal slight hyperintensity of the plexus components (arrow). The hyperintense gluteal vessels are seen lateral to the plexus (arrowhead).*
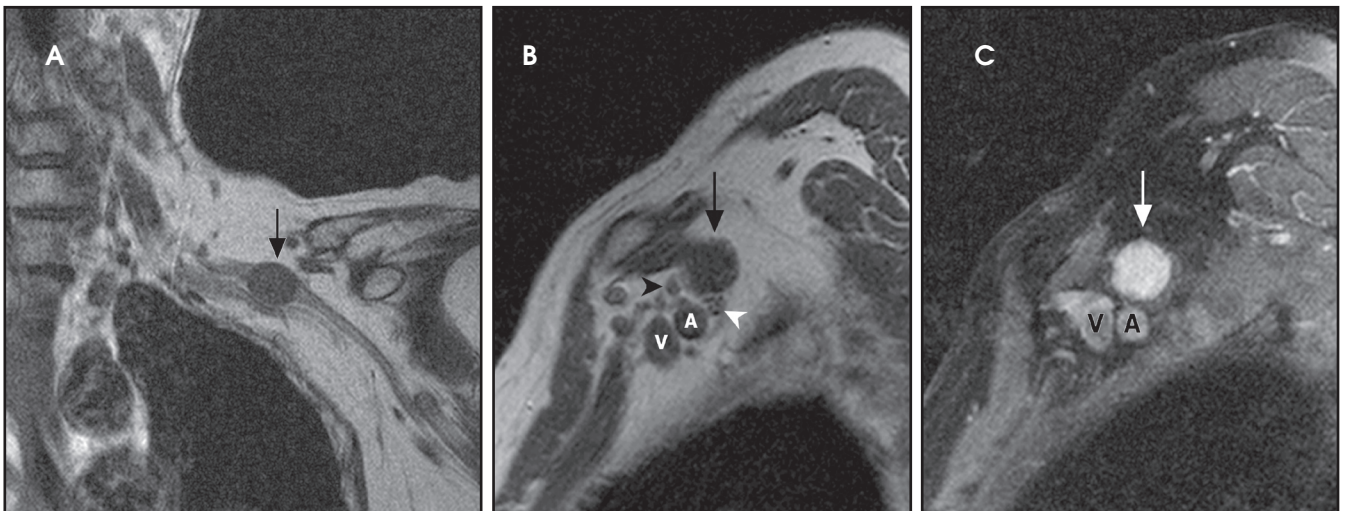

FIGURE 5. *Schwannoma of the posterior cord. (A) Coronal T1W image shows a sharply marginated oval-shaped mass (arrow) contiguous with the left brachial plexus in the region of the cords. Sagittal T1W image (B) shows the mass (arrow) superior to the "flow void" of the axillary artery-A, posterior to the vein- V, and in between the lateral (black arrowhead) and medial (white arrowhead) cords correspond in location to the posterior cord. On postcontrast fat-saturated T1W image (C), the mass enhances homogenously (arrow).*

give rise to the different branches, the largest of which is the sciatic nerve. The plexus is located anterior to the piriformis muscle and the sacroiliac joint. The sciatic nerve exits the pelvis through the greater sciatic foramen along with the piriformis muscle and the superior and inferior gluteal vessels and nerves. The sciatic nerve courses laterally in the gluteal region and then inferiorly in the posterior portion of the upper thigh. The superior gluteal vessels and nerve exit the pelvis in the superior aspect of the greater sciatic foramen. The inferior gluteal vessels and nerve accompany the sciatic nerve through the greater sciatic foramen and are located posteromedial to it[1] (Figure 2).

MR Imaging technique

The brachial plexus presents an imaging challenge due to its complex anatomy and close proximity to the lungs and major vessels, where there are often magnetic susceptibility effects. To obtain high-quality images with high signal-to-noise ratio (SNR), dedicated phased-array radiofrequency (RF) receiver coils are routinely used.[4] Evaluation of the brachial plexus requires flow-compensated, T1- and T2-weighted images. The T1-weighted images display regional anatomy, including the various muscles, blood vessels, and nerves outlined by tissue fat planes. T2-weighted images are used to detect pathologic changes within the nerves. Since nerves are small, the abnormal signal within the plexus can be obscured by signals from adjacent fat. To overcome this problem, various methods of fat suppression are
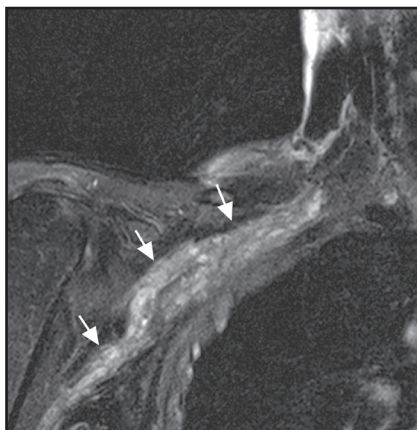
FIGURE 6. *Neurofibromatosis Type 1. Coronal fat-suppressed T2W images show fusiform enlargement of the right brachial plexus (arrows) and hyperintense signal.*
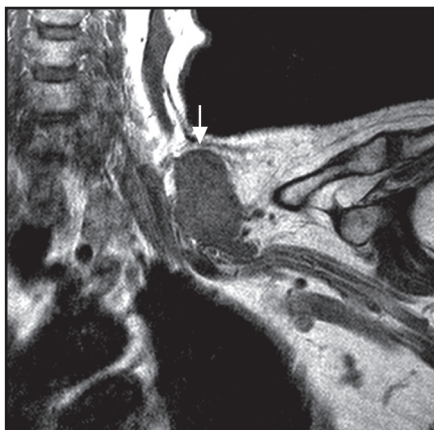

FIGURE 7. *Coronal T1W image in a patient with adrenal carcinoma metastatic to the brachial plexus. A lobulated, ill-defined mass is noted in the left supraclavicular region (arrow) invading the divisions of the brachial plexus.*
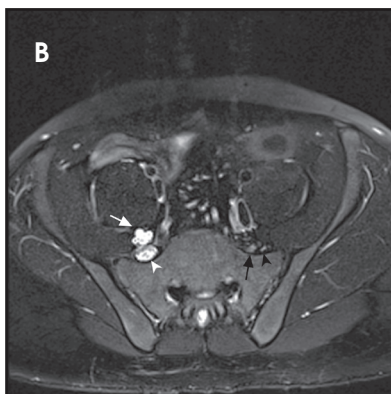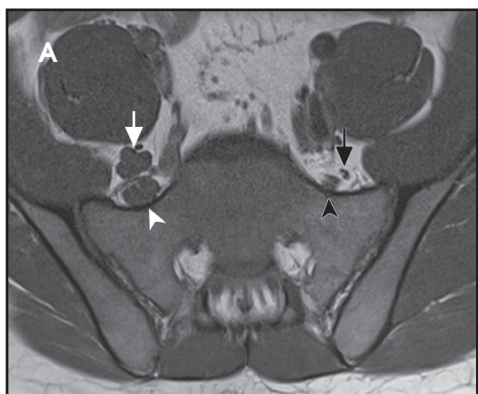

FIGURE 8. *Hypertrophic neuropathy. Axial T1W image (A) and T2W image with fat suppression (B) show diffuse enlargement and increased signal of the right L4 (white arrow) and L5 (white arrowhead) roots compared to the contralateral L4 (black arrow) and L5 (black arrowhead) roots.*
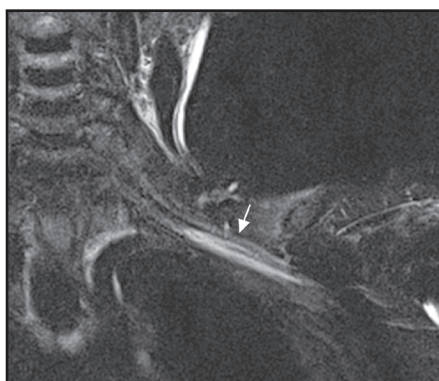

FIGURE 9. *Stretch injury secondary to positioning for a surgical procedure. MR imaging was performed 2 weeks after surgery for retrosternal goiter resection where the arm was positioned above the patient head for 6 hours. Coronal T2W image with fat suppression shows diffuse hyperintense signal (arrow) in the lower trunk, divisions and cords of the left brachial plexus.*
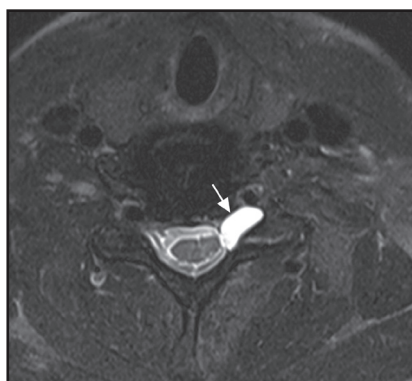

FIGURE 10. *Traumatic pseudomeningocele. 30-year-old man hit by car while riding his bike 6 months before MR imaging. Axial T2W image with fat suppression shows a pseudomeningocele (arrow) at the site of complete avulsion of the left C7 nerve root.*

used. The 2 most common methods are frequency-selective saturation of the fat resonance, and short tau inversion recovery (STIR), with nulling of the signal contribution from fat. Each method has advantages and disadvantages. Because bulk susceptibility artifacts are especially difficult to overcome when imaging the base of the neck,[5] the STIR method is often preferred. The advantage of STIR is that it gives uniform and consistent suppression of fat signal while maintaining excellent T2 contrast.[2] There are, however, two disadvantages to the STIR method. The first is relatively low SNR. The second is greater sensitivity to blood flow artifacts that can degrade the resulting STIR image. A spatial presaturation band is placed over the heart and aortic root to reduce the intensity of these artifacts. In addition, respiratory compensation is often added to the imaging sequence to lessen respiratory motion phase-encoding artifacts. Chemical shift fat suppression is usually successful in the lumbar and pelvic region, and is typically used for T2W imaging of the sacral plexus. The field of view for plexus imaging is 24 cm to 26 cm, and a 512×256 or 512×512 matrix is used. For brachial plexus imaging, the FOV is targeted to the side of clinical interest. If necessary, an initial image with larger FOV, demonstrating both symptomatic and asymptomatic sides, may be obtained with the body coil. Images of the brachial plexus are obtained in two orientations. In-plane images (parallel to the long axis of the plexus) are acquired contiguously in the direct coronal plane using a slice thickness of 4 mm. Cross-sectional images (perpendicular to the long axis of the plexus) are performed using a sagittal plane (Figure 3). For in-plane and cross-sectional images of the sacral plexus, both sides are included in the FOV. Cross sectional images are acquired with a 2 mm to 4 mm gap between slices to achieve adequate coverage in a reasonable scan time (Figure 4).

Contrast-enhanced images are obtained routinely in patients following surgery and being evaluated for suspected neoplasm, radiation injury,
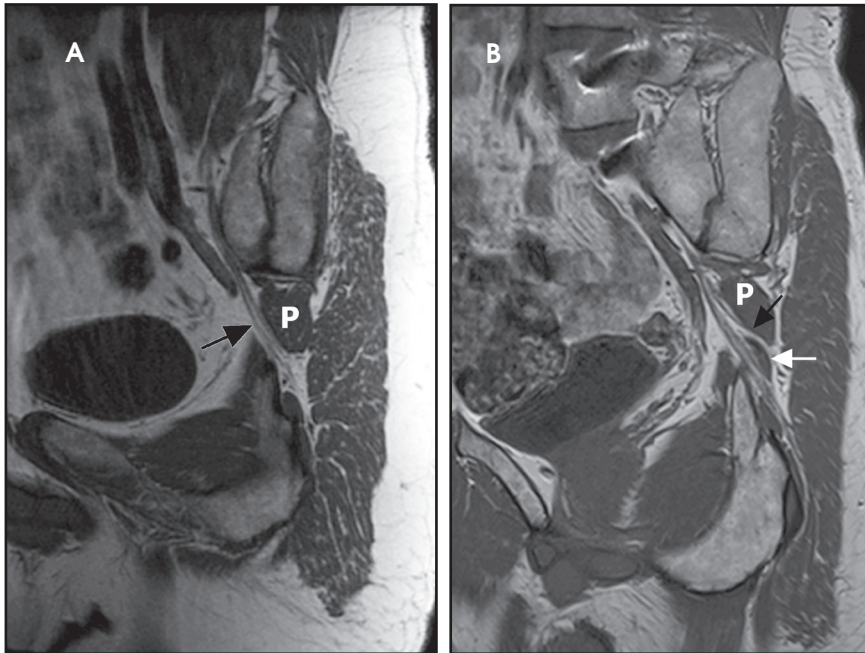
FIGURE 11. *Piriformis syndrome. Oblique coronal T1W images obtained perpendicular to the piriformis muscle (P) demonstrating the normal sciatic nerve (arrow) exiting the greater sciatic foramen anterior to the piriformis muscle (A). Images of another patient (B) show the bifid tendon (white arrow) of the piriformis muscle (P). A portion of normal sciatic nerve (black arrow) is seen passing through the bifid tendon. The nerve is normal in thickness and signal intensity but is predisposed for compression with internal rotation of the hip.*
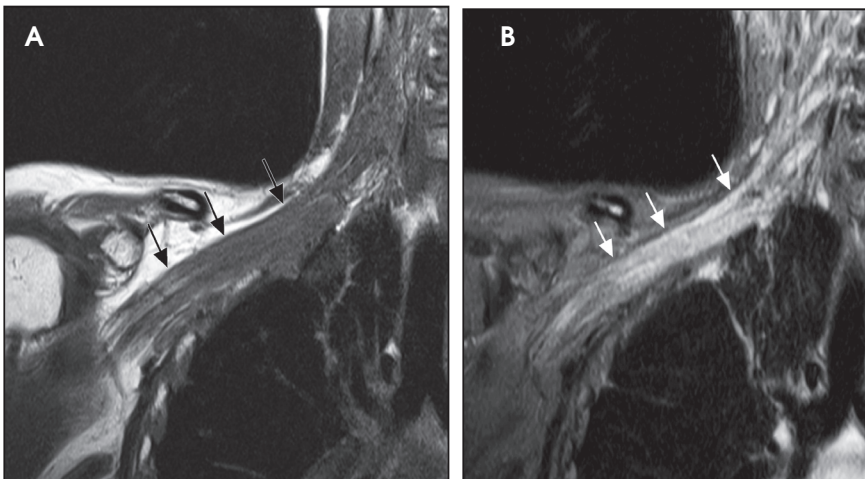

FIGURE 12. *Radiation injury. The patient with history of breast carcinoma presented with signs and symptoms of progressive plexopathy 2 years after radiation therapy to the right supraclavicular region and axilla. Coronal T1W (A) image shows uniform diffuse enlargement of the roots, trunks and divisions of the right brachial plexus (arrows). On the STIR image (B), the plexus structures are markedly hyperintense (arrows).*

inflammation or abscess formation. In addition to these indications, contrast-enhanced images have also proven useful in some cases of nerve entrapment and stretch injury. In cases of acute severe traumatic nerve injury and simple compressive neuropathy, a noncontrast exam is usually sufficient.

For contrast-enhanced studies, a standard dose of 0.1 mmol/kg is administered as an intravenous bolus. T1-weighted spin-echo images, with frequency-selective fat saturation, are acquired immediately following injection. In some cases, delayed imaging, 10 to 20 minutes postinjection, may be

useful to better define abnormal areas of enhancement.

T1-weighted, T2 with fat suppression or STIR, and contrast-enhanced T1 fat-saturated images are obtained in precisely the same plane of orientation and using the same imaging parameters in terms of slice thickness, FOV and location. The resulting images are co-registered and, thus, directly comparable. This is necessary since the fat-suppressed images usually will not adequately demonstrate normal tissue planes (outlined by fat), making identification of anatomical landmarks more difficult. T1-weighted images are used to identify the plexus using anatomical landmarks. The radiologist must then rely on direct comparison between the T1-weighted, STIR, and contrast-enhanced images for accurate identification of signal abnormality, abnormal enhancement thickening, or masses evolving the plexus.

Pathologic conditions

Indications for imaging of the plexus include evaluation of neoplastic or inflammatory mass, traumatic injury, entrapment or nontraumatic compressive lesions, and distinguishing radiation injury from recurrent tumor.

Mass involving the plexus

A tumor may present as a mass intrinsic or extrinsic to plexus components. MRI provides valuable information that aids in preoperative planning. Primary tumors involving the plexus include nerve sheath tumors. Schwannoma (Figure 5) is typically an eccentric mass involving one plexus component while plexiform neurofibromas (Figure 6) are usually multiple and may diffusely enlarge many components of the plexus. Other tumors may invade the plexus by direct extension, such as superior sulcus tumor (Pancoast tumor), breast carcinoma, retroperitoneal or intraperitoneal tumors and lymphoma. Metastatic lesions (Figure 7) and benign processes, such as aggressive fibromatosis (desmoid tumor), endometriosis or nodular fasciitis, may also involve the plexus.[6]

Inflammatory/idiopathic conditions

Acute plexitis is an uncommon disorder. A viral etiology has been proposed while some cases have been reported to occur following vaccinations.[7] Hypertrophy and diffuse hyperintensity on T2W images of the plexus components have been described in cases of chronic inflammatory demyelinating polyneuropathy (CIDP), multifocal motor neuropathy (MMN), and hereditary hypertrophic motor and sensory neuropathy (HMSN). CIDP (Figure 8) is an immune mediated neurological disorder causing damage to the myelin sheath of the peripheral nerves. Radiologic characteristics include diffuse marked enlargement of peripheral nerves. Gadolinium enhancement may be present in active disease.[8,9]

Traumatic injury

Blunt or penetrating trauma with fracture, dislocation, or hematoma formation may produce compression stretching or avulsion of the brachial plexus. Stretch injury appears as long diffuse involvement (Figure 9). Nerve root avulsion may result with dural tear forming traumatic pseudomeningocoele seen as a focal CSF collection extending from the neural foramen (Figure 10). Occasionally, posttraumatic neuroma may develop. In the sacral plexus, nerve compression may result from retroperitoneal or psoas hematoma.

Entrapment or nontraumatic compressive lesions

In evaluation of the brachial plexus, various forms of thoracic outlet syndrome may be a cause of entrapment. Examples include entrapment of the lower trunk at the insertion of the anterior scalene muscle on the first rib (scalenus anticus syndrome), entrapment by a crossing cervical rib (cervical rib syndrome),[10] and compression by subclavian artery aneurysm. In the sacral plexus, entrapment of the sciatic nerve at the greater sciatic foramen (piriformis syndrome) may be secondary to asymmetry of the piriformis muscle size or anatomic variations in the course of the sciatic nerve relative to the piriformis muscle (Figure 11).[11] Obtaining a sequence perpendicular to the piriformis muscle is crucial in identification of these anatomic variants.

Post-treatment evaluation

Patients with a history of cancer and radiation therapy may have recurrent tumor or radiation-induced plexopathy. Radiation fibrosis may occur several months to years after the completion of therapy. Findings of radiation fibrosis include uniform thickening, enhancement and diffuse T2 hyperintensity of the plexus nerves within the radiation field or low T1 and T2 soft-tissue changes.[6,12] The absence of focal or eccentric mass distinguishes radiation plexopathy from recurrent tumor (Figure 12).[13]

Conclusion

High-resolution MR imaging of the brachial and sacral plexus provides important information used to determine the need for biopsy or surgical planning and treatment, if necessary. In cases of traumatic injury, MR imaging is helpful in assessing the need for surgical repair and in following recovery of these nerves postoperatively.

REFERENCES

1. Bowen BC, Maravilla KR, Saraf-Lavi E. Magnetic Resonance Imaging of the peripheral nervous system, Chapter 73. In: Latchaw RE, Kucharczyk J, Moseley ME, eds. *Imaging of the Nervous System. Diagnostic and Therapeutic Applications, Vol 2.* Philadelphia, Pa: Elsevier Mosby; 2005:1479-1497.
2. Maravilla KR, Bowen BC. Imaging of the peripheral nervous system: Evaluation of peripheral neuropathy and plexopathy. *AJNR Am J Neuroradiol.* 1998;19:1011-1023.
3. Bowen BC. Brachial plexus. In: Stark DD, Bradley WG, eds. *Magnetic Resonance Imaging.* 3rd ed. St Louis, Mo: Mosby; 1999:1821-1832.
4. Hayes CE, Hattes N, Roemer PB. Volume imaging with MR phased arrays. *Magn Reson Med.* 1991;18:309-319.
5. Cox I, Dillon WP. Low-cost device for avoiding bulk susceptibility artifacts in chemical-selective fat saturation MR of the head and neck. *AJNR Am J Neuroradiol.* 1995;16:1367-1369.
6. Wittenberg KH, Adkins MC. MR imaging of nontraumatic brachial plexopathies: Frequency and spectrum of findings. *Radiographics.* 2000;20: 1023-1032.
7. Miller JD, Pruitt S, McDonald TJ. Acute brachial plexus neuritis: An uncommon cause of shoulder pain. *Am Fam Physician.* 2000;62:2067-2072.
8. Duggins AJ, McLeod JG, Pollard JD, et al. Spinal root and plexus hypertrophy in chronic inflammatory demyelinating polyneuropathy. *Brain.* 1999;122:1383-1390.
9. Beydoun SR, Muir J, Apelian RG, et al. Clinical and imaging findings in three patients with advanced inflammatory demyelinating polyradiculoneuropathy associated with nerve root hypertrophy. *J Clin Neuromuscul Dis.* 2012;13:105-112.
10. Panegyres PK, Moore N, Gibson R, et al. Thoracic outlet syndromes and magnetic resonance imaging. *Brain.* 1993;116:823-841.
11. Russell JM, Kransdorf MJ, Bancroft LW, et al. Magnetic resonance imaging of the sacral plexus and piriformis muscles. *Skeletal Radiol.* 2008;37: 709-713.
12. Bowen BC, Verma AH, Brandon A, Fiedler JA. Radiation-induced brachial plexopathy: MR and clinical findings. *AJNR Am J Neuroradiol.* 1996;17:1932-1936.
13. Thyagarajan D, Cascino T, Harms G. Magnetic resonance imaging in brachial plexopathy of cancer. *Neurology.* 1995;45:421-427.